THE ASTROPHYSICAL JOURNAL, 317:593–600, 1987 June 15

ARE THE VIRIAL MASSES OF CLUSTERS SMALLER THAN WE THINK?

L. L. COWIE
Space Telescope Science Institute
AND
M. HENRIKSEN AND R. MUSHOTZKY
NASA/Goddard Space Flight Center
Received 1986 February 4; accepted 1986 November 21

ABSTRACT

We consider the constraints that the available X-ray spectral and imaging data place on the mass distribution and mass-to-light ratio of rich clusters. We find for the best determined cases that the mass-to-light ratio is less than 125 h_{50} at radii exceeding 1 h_{50}^{-1} Mpc. The mass-to-light ratio is approximately constant at radii exceeding 1 h_{50}^{-1} Mpc but may rise to values of roughly 200 h_{50} in the central regions. The fraction of the total mass that is in baryons, primarily the hot X-ray emitting gas, is roughly 30%, thus setting the mass-to-light ratio of the "dark" material to roughly 70. The model that fits the X-ray data for Coma is in good agreement with the observed optical velocity dispersion versus radius data.

Subject headings: cosmology—galaxies: clustering—galaxies: X-rays

I. INTRODUCTION

It has become a part of the astrophysical lore to suppose that the virial masses in the rich clusters are large. Typical mass-to-light ratios (M/L_V, where L_V is the visual luminosity) are generally supposed to lie between (200 and 300) h_{50}[1] (for a recent review see Rood 1981). This missing mass (or missing light) problem fits neatly into a strongly held picture that the mass-to-light ratio increases with scale size of the bound system, and that the universe is closed, as required by the inflationary cosmologies. Of course, even the large mass-to-light ratios of clusters of 300 h_{50} is too low a value to provide the closure M/L ratio of (500–1000) h_{50} (Felten 1985, 1986). However, as is well known, the basis for these views is very fragile. Detailed optical data on light profiles and velocity dispersions as functions of radius are available for only a few clusters (cf. Kent and Gunn 1982; Kent and Sargent 1983). Even where such data do exist, translation into a virial mass profile requires many assumptions, including spherical symmetry, constant mass-to-light ratios, details of the distribution functions of the galaxies (the form of the orbits, e.g., radial vs. symmetric, the assumption of relaxation of the galaxies in the potential), and the form of the potential. The final answer is quite sensitive to many of these assumptions. For example, Bailey (1982) has shown that breaking the constant M/L_V requirement and allowing the virial mass to be centrally concentated allows the total mass to be reduced: M/L_V could be as low as 50 h_{50} in the Coma Cluster in such models. If we can demonstrate that this type of model is preferred, the impact on our cosmological viewpoint should be profound.

One of the ways to test this question is through study of the X-ray atmospheres of the clusters. Determining total mass-to-light ratios in clusters using observations of the X-ray emitting gas should hold many advantages over traditional optical methods. The gas is guaranteed to have an isotropic velocity distribution and to be quasi-static in the inner cluster (e.g., Cavaliere 1980). Thus integration of the hydrostatic equation can allow a direct measurement of the run of the total cluster mass. The reason such determinations have not been seriously pursued, as yet, is that it is generally assumed that both gas density and temperature profiles must be well known to use the method (e.g., Sarazin 1985), and at present only the gas density profiles are available from the *Einstein* Imaging data (Jones and Forman 1984). There have been attempts to measure the mass of galaxies where both density and temperature information is available; the most notable application is to M87 (Fabricant and Gorenstein 1983). However, as we shall show in this paper, the density profile data alone, when combined with integral information, can provide very strong constraints on cluster virial masses even without the full temperature profile.

Emission measure weighted spectra for many clusters are available from *OSO 8*, *Ariel V*, and *HEAO 1* data, and for the past few years these spectra have been approximated by isothermal bremsstrahlung emission (e.g., Mushotzky 1984). However, recent analyses (Henriksen and Mushotzky 1986*b*) have shown that such single-temperature models are not good fits to a number of clusters. In these cases a range of temperatures is required, including material at both higher and lower temperatures than would be inferred from an isothermal fit. Henriksen and Mushotzky analyzed this data in terms of a polytropic equation of state which allows a simple two-parameter fit to the data. They then used this fit to measure virial masses in clusters with the hydrostatic equation and concluded that the virial masses were considerably lower than previously estimated.

After summarizing the necessary background material in § II, we generalize this procedure in § III and show that within such a polytropic model a value of the mass-to-light ratio $M/L_V \approx 125\ h_{50}$ at $R = 2\ h_{50}^{-1}$ Mpc for both Coma and Perseus clusters is entirely consistent with all the available optical and X-ray data.

However, the assumption of the polytropic equation of state may be considerably too specific, and in § IV we consider an alternative procedure. In this section we assume that the mass-to-light ratio is constant in the clusters (an assumption familiar from previous analysis but still not a necessary assumption)

[1] h_{50} is the Hubble constant in units of 50 km s^{-1} Mpc^{-1}.

and that the light profile is given by an analytic King model (which except in the central regions of Coma seems to be an adequate representation of the data; Quintana 1979). Knowing the virial mass profile and the density profile, we can use the hydrostatic equation to obtain the temperature profile as a function of three parameters—the mass-to-light ratio, the optical core radius, and the asymptotic temperature. We can then construct the integrated spectrum. We find that this model *cannot* provide an adequate fit to the spectra, but invariably gives too isothermal a temperature profile. Inclusion of a large central mass in the cluster core ($\sim 2 \times 10^{13}\ M_\odot$) allows us to obtain agreement with the spectral data, but when this is done the required M/L ratio outside the core again falls to low values ($\leq 125\ h_{50}$). Preferred values are typically around 60 $h_{50}{}^{+1}$.

Finally, we show in § V that there are models which provide an adequate fit to the optical as well as the X-ray data, and that these models generally give $M/L_V \approx 100\ h_{50}$, beyond $0.5\ h_{50}{}^{-1}$ Mpc.

In § VI we summarize our conclusions and consider the implications of our results.

II. BACKGROUND MATERIAL

a) *Gas Density Profiles*

The Imaging Proportional Counter (IPC) aboard the *Einstein Observatory* obtained X-ray surface brightness profiles for many clusters out to radii of roughly 1 Mpc (cf. Abramopoulos and Ku 1983; Jones and Forman 1984). For a spherically symmetric atmosphere, the surface brightness $S(r)$ at projected radius r is related to the emission per unit volume into the IPC passband $E(R)$ at radius R by the equation

$$S(r) = \frac{1}{2\pi} \int_r^\infty \frac{E(R) R dR}{(R^2 - r^2)^{1/2}} . \tag{1}$$

This Abel equation can be inverted to give

$$E(r) = \frac{4}{r} \frac{d}{dr} \int_r^\infty \frac{R S(R) dR}{(R^2 - r^2)^{1/2}} \tag{2}$$

as noted by Cavaliere (1980). Direct inversion of equation (2) without additional external constraints is quite unstable (the deconvolution technique used by Fabian *et al.* 1981 and Stewart, Canizares, and Nulsen 1984 is equivalent to inversion of this equation with additional constraints on the potential, total X-ray flux, and mean X-ray temperature). The simplest procedure, fitting a smooth function to the data prior to inversion, does retain most of the available information in the surface brightness profile. As Jones and Forman have shown, the surface brightness profiles are well fitted, outside the central core, by a law of the form

$$S(r) = S_0[1 + (r^2/a^2)]^{1/2 - 3\beta} . \tag{3}$$

This functional form was originally derived for the case of an isothermal gas and isothermal cluster (Cavaliere and Fusco-Femiano 1976), but this interpretation is not consistent with the optical velocity dispersions, optical size properties, and the X-ray spectral data (Mushotzky 1984). As will be clear from our later discussion, equation (3) is best considered as an extremely good empirical fit to the surface brightness. Equation (3) may now be inverted, using equation (2) subject to the assumption of spherical symmetry, to give an emission per unit volume

$$E(r) = 4\pi^{1/2} \frac{\Gamma(3\beta)}{\Gamma(3\beta - 1/2)} \left(\frac{S_0}{a}\right) \left(1 + \frac{r^2}{a^2}\right)^{-3\beta} . \tag{4}$$

In this equation, $E(r) = n_e{}^2 \epsilon(T)$, where $\epsilon(T)$ is the emissivity of the gas convolved through the *Einstein* IPC passband (and Γ is the gamma function). Numerical integration of a thin bremsstrahlung spectrum through the effective area of the IPC as a function of energy shows that ϵ is a weak function of temperature dropping roughly as $(T^{-0.40})$ (e.g., Fabricant, Lecar, and Gorenstein 1980; Fabian *et al.* 1981) at temperatures greater than 2 keV. Thus ϵ is almost entirely dependent on density. In particular, if the gas is described by a polytropic equation of state $T \approx n^{\gamma - 1}$, then the density profile may be written

$$n = n_0[1 + (r^2/a^2)]^{-\delta} , \tag{5}$$

where

$$\delta \approx \tfrac{3}{2}\beta/[1 - 0.20(\gamma - 1)] . \tag{6}$$

Jones and Forman found a maximal range of β of 0.40 to 0.83 using extremal error bars (with a minimum range of 0.52 to 0.68) over their cluster sample which translates to $\delta = 0.60 \rightarrow 1.25$ for $\gamma = 1$ and $\delta = 0.54 \rightarrow 1.11$ for $\gamma = 5/3$. The δ ranges and other X-ray parameters for the five clusters we shall consider here are summarized in Table 1.

As Forman and Jones note, a number of clusters are not well fitted by equation (4) within the core regions. These are generally the clusters which have cooling flows inside the core. Clusters, such as Coma, which do not have such flows are generally well fitted throughout.

The density deconvolution outside the core does not, of course, depend in detail on the core properties. The density deconvolution is also not sensitive to the details of the fit to the surface brightness or to the symmetry assumption. In particular, as Fabian *et al.* (1981) and Rybicki, Gorenstein, and Fabricant (1984) have shown, if the clusters are cylindrically symmetric and the ellipticity is not too high, the density profiles do not differ radically from those obtained assuming spherical symmetry. Further, much of this weak symmetry dependence cancels out in virial mass determinations.

b) *Temperature Information*

The integrated emission from the cluster is dominated by emission from the regions where the density profile is determined by the *Einstein* measurements. Temperatures based on the isothermal models for the *HEAO 1* data are given in Table 1, under the column labeled T_{ISO}, but such models do not generally provide an adequate fit. More generally, the spectra

TABLE 1

POLYTROPIC MODEL PARAMETERS

Cluster	δ	T_{ISO}[a] (keV)	T_0[b] (keV)	γ
A85	0.9–0.98[c]	6.8 ± 0.5[d]	12.8–22.5[e]	1.3–1.66
A426	0.83–0.90[c]	6.4 ± 0.4[d]	7.6–10.8[e]	1.15–1.36
A1656	1.00–1.30[f]	8.0 ± 0.4[g]	15.3–20[g]	1.38–1.6
A1795	0.98–1.20[c]	$6.5^{+0.5}_{-0.3}$[d]	10.2–21[e]	1.25–1.66
A2199	0.95–1.10[e]	3.6 ± 0.6[d]	4–9.5[e]	1.0–1.5

[a] Temperature if the gas is isothermal.
[b] Central temperature in keV.
[c] Jones and Forman 1984.
[d] Mushotzky 1984.
[e] Henriksen and Mushotzky 1986*b*.
[f] Abramopoulos, Chanan, and Ku 1981.
[g] Henriksen and Mushotzky 1986*a*.

may be fully specified by the differential volume emission measure as a function of temperature. A function of the form

$$E(T)dT = A\left(\frac{T}{T_0}\right)^u\left[1-\left(\frac{T}{T_0}\right)^w\right]^{1/2}\frac{dT}{T_0} \quad (7)$$

does provide an acceptable *fit* to the *HEAO 1* data. Equation (4) is obtained for the particular case of a polytropic equation of state $T/T_0 = (n/n_0)^{\gamma-1}$ and the density profile of equation (5) with

$$A = \frac{2\pi a^3 {n_0}^2}{\phi}, \quad (8a)$$

$$u = \frac{(3-\gamma)\delta - 1.5}{\phi}, \quad (8b)$$

and

$$w = \frac{1}{\phi}, \quad (8c)$$

where $\phi = \delta(\gamma - 1)$. The value of w is extremely poorly constrained by the observations; if it is force-fitted to a typical value of ~ 3, then the values of T_0 and γ (where the ranges indicate 95% confidence limits) for a number of clusters are those given in Table 1. Both T_0 and n would be much more tightly constrained by the extreme high signal-to-noise ratio of the *HEAO 1* data but for the almost featureless form of the spectra. Unfortunately, variations in T_0 can be compensated for by changes in n or equivalently γ. This may be seen intuitively by noting that a mixture of higher and lower temperature material is hard to distinguish from an intermediate-temperature gas when only a limited spectral coverage is available. Correspondingly the 95% confidence region in (γ, T) space is essentially a line and the value of T_0 is a monotonically increasing function of γ. ($T_0 \approx \gamma^2$ is a good approximation for these clusters.) Thus the two 95% confidence ranges should not be treated independently.

The preferred temperature profiles are generally quite shallow and in some cases (e.g., A2199) could be close to isothermal. Coma has one of the steepest slopes, and here the temperature must vary by about a factor of 2–3 within the radius where 90% of the flux originates. For the polytropic case with $\gamma = 1.4$ and $\delta = 1$, the temperature in Coma falls from 17 keV at the center to 8.8 keV at 2 core radii and 4.6 keV at 5 core radii, if $\gamma = 1.25$ the temperature varies from 15.3 keV at the center to 10.2 keV at 2 core radii and 6.8 keV at 5 core radii. An isothermal model by contrast (Table 1) gives a best-fit temperature of ~ 8 keV (Henriksen and Mushotzky 1986*a*). It is possible, that the best-fit value of γ may be changed by the presence of the strong cooling flow in A85, A426, A1795, and A2199. However, it is unlikely that the presence of the cooling flow will change the value of the derived central temperature. Given that the cluster without a cooling flow, Coma, has the highest allowed value of γ, it may be possible that the cooling flow to some extent hides the signature of a higher γ polytropic model.

c) *Hydrostatic Balance*

The hydrostatic equation in a spherically symmetric cluster may be written as (e.g., Fabricant, Lecar, and Gorenstein 1981)

$$M_V(r) = \frac{-kTr}{G\bar{m}}\left(\frac{d\ln n}{d\ln r} + \frac{d\ln T}{d\ln r}\right), \quad (9)$$

where M_V is the virial binding mass as a function of radius, T is the temperature, n is the density profile, and $\bar{m}$ is the mass per gas particle. With a density profile of the form of equation (5) this may be rewritten as

$$M_V(r) = \frac{ka}{G\bar{m}}\,Tx\left[\frac{2\delta x^2}{(1+x^2)} - \frac{d\ln T}{d\ln r}\right], \quad (10)$$

where for simplicity we have defined $x = r/a$, where a is the gas core radius. For a polytropic equation of state, this simplifies still further to

$$M_V = 2\gamma\delta\,\frac{kaT_0}{G\bar{m}}\,\frac{x^3}{(1+x^2)^{1+\phi}}, \quad (11a)$$

where T_0 is the central temperature. Putting in typical values for the parameters and substituting we find

$$M_v = 1.92\times 10^{14}\delta\gamma(T_0/10)_{\rm keV}(a/0.25)_{\rm Mpc} \times x^3(1+x^2)^{-(1+\phi)}\,M_\odot. \quad (11b)$$

The ratio of the "polytropic" to "isothermal" binding mass at large radii is

$$\frac{M_v(\gamma)}{M_v({\rm iso})} = \gamma x^{-2\phi} \quad (11c)$$

which for "typical" values of the parameters (see § III) is

$$\frac{M_v(\gamma)}{M_v({\rm iso})} \sim 1.25x^{-1/2}.$$

III. POLYTROPIC EQUATION OF STATE

a) *General Description*

We must always recognize that a polytropic equation of state corresponds to a particular choice of temperature profile which may force us to conclusions which can be avoided in a freer model. However, the simplification of such a parameterized fit allows analytic descriptions and gives considerable insight.

Equations (7) and (11) provide the basic equations for this section. For a given cluster we may use the following procedure. First, the range of acceptable δ is determined from the IPC data on the cluster. Generally δ lies around 1 and fits extend from slightly less than 1 h_{50}^{-1} Mpc to about $2\frac{1}{2}$ h_{50}^{-1} Mpc (Jones and Forman 1984). For each value of δ a range of γ and $T_0(\gamma)$ is determined, using equation (7) in conjunction with the *HEAO 1* data, as summarized in Table 1. Finally the run of virial mass and the range of the determinations can be found from equation (11).

Before proceeding to analyze specific cases, some general points follow at once from the functional form of equation (11). The density corresponding to this mass profile is given by

$$\rho = \left(\frac{\gamma\delta}{2\pi Ga^2}\right)\frac{kT_0}{\bar{m}}\left[\frac{3-(2\phi-1)x^2}{(1+x^2)^{(\phi+2)}}\right]. \quad (12)$$

From equation (12) we can see that for $2\phi \geq 1$, the virial density falls to zero at a finite value

$$x_{\rm max} = \left(\frac{3}{2\phi-1}\right)^{1/2}. \quad (13)$$

A cutoff in the virial density at such small radii (typically about 2 core radii) is not acceptable since both gas and galaxy light

extend beyond this point. Thus, we must impose the condition that

$$\delta(\gamma - 1) \equiv \phi \leq \tfrac{1}{2} \tag{14}$$

so that there is no "natural cutoff" at a few core radii.

This constraint should be viewed as an empirical relation. Gas obeying the form of equation (5) must have a low polytropic index to extend to even moderate radii.

The physical constraint on ϕ favors lower values of δ and shallower slopes (smaller γ) as can be seen from Table 1. Coma pushes hardest on this constraint. The best-fit δ (1.15) even with the lowest allowed value of γ (1.4) would give $\phi = 0.46$ which would result in a very rapid mass drop beyond the core radius.

If we adopt an analytic "King" approximation to the cluster light profile

$$\rho_L = \rho_{L_0}\left(1 + \frac{r^2}{b^2}\right)^{-3/2}, \tag{15}$$

(where ρ_L is the density of light from the cluster) then we may write the M/L ratio as a function of position

$$\frac{\rho_v}{\rho_L} = \frac{(\phi + \delta)}{2\pi G a^2 \rho_{L_0}} \frac{kT_0}{\bar{m}} \left[\frac{3 - (2\phi - 1)x^2}{(1 + x^2)^{\phi+2}}\right](1 + B^2x^2)^{3/2}, \tag{16}$$

where $B^2 = a^2/b^2$ is the square of the ratio of X-ray to optical core radii. As opposed to previous treatments we do not require the *mass* profile to follow the "King" light profile, and we adopt this form for ease of comparison with previous work.

b) Global Mass and M/L

The virial mass at larger radii is maximized if we adopt the lowest acceptable values of δ and γ and the largest acceptable X-ray core radius (Table 2). The maximum mass profiles for the five clusters of Table 2 are shown in Figure 1 together with the corresponding M/L_V profiles for Coma and Perseus. In computing the mass-to-light profiles we have used King model fits to the light distribution of the form of equation (15) with the optical core radius $b = 0.37\ h_{50}^{-1}$ Mpc and L_V (inside 7 h_{50}^{-1} Mpc) $= 1.6 \times 10^{13}\ h_{50}^{-2}\ L_\odot$ for Coma (Kent and Gunn 1982) as modified in Kent and Sargent (1983), and $b = 0.34\ h_{50}^{-1}$ Mpc and L_V (inside 5.6 h_{50}^{-1} Mpc) $= 1.1 \times 10^{13}\ h_{50}^{-2}\ L_\odot$ for Perseus (Kent and Sargent 1983). The corresponding visual luminosity profiles are

$$L_V(\lesssim y) = 6.2 \times 10^{12}\ h_{50}^{-2} f(y), \quad \text{(Coma)} \tag{17a}$$

$$L_V(\lesssim y) = 4.4 \times 10^{12}\ h_{50}^{-2} f(y), \quad \text{(Perseus)} \tag{17b}$$

where $y = r/b$ and

$$f(y) = \ln\left[y + (1 + y^2)^{1/2}\right] - y/(1 + y^2)^{1/2}. \tag{18}$$

The visual luminosity inside $2\ h_{50}^{-1}$ Mpc is $8.7 \times 10^{12}\ h_{50}^{-2}\ L_\odot$ (Coma) and $6.5\ 10^{12}\ h_{50}^{-2}\ L_\odot$ (Perseus). Abell (1977) gives the visual luminosity in Coma out to a radius of $8.6\ h_{50}^{-1}$ Mpc as $(1.6\text{–}2.75) \times 10^{13}\ L_\odot$. Using his normalization would change the normalization of the total luminosity in Coma to $(6.8\text{–}11.7) \times 10^{12}$ rather than $6.2 \times 10^{12}\ L_\odot$ and result in even lower values of M/L_v.

Even with these extreme parameters (lowest allowable γ and δ), the M/L ratio (using Kent and Gunn's values) is only

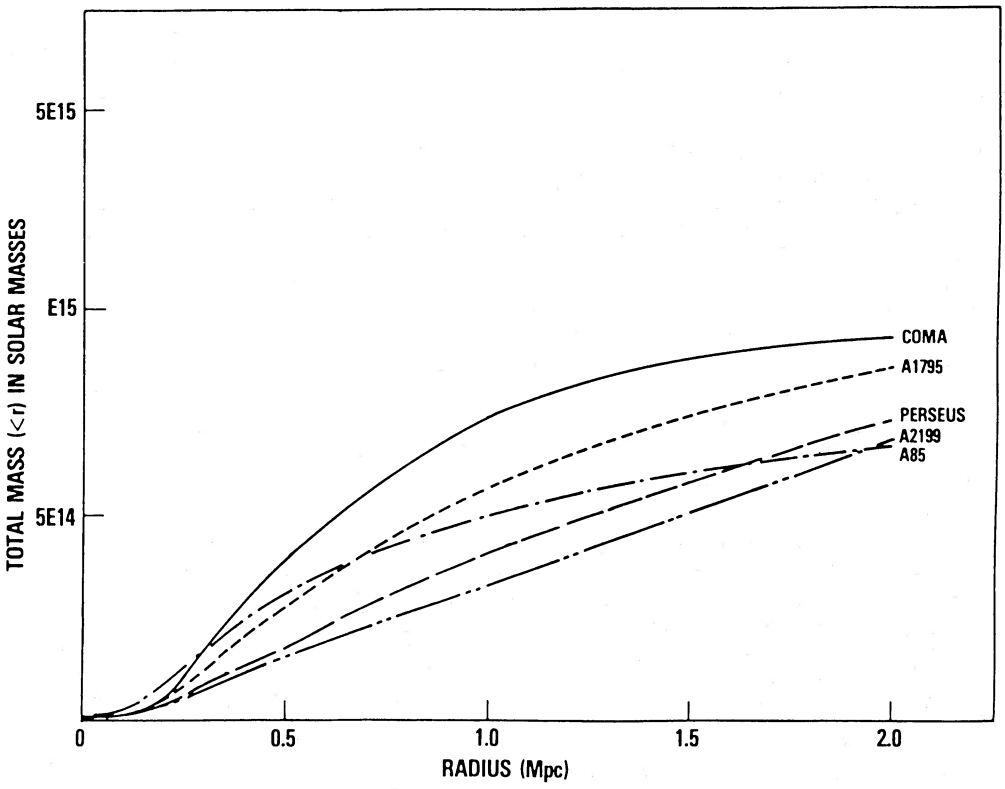

FIG. 1.—The maximum virial mass as a function of radius for the five clusters. These values are obtained for the maximum δ core radius pair. These values are obtained from Jones and Forman (1984).

TABLE 2

MAXIMAL BINDING MASSES

Cluster	Core Radius Range[a]	Maximal Mass[b]
A85	0.19–0.26	6.7
A426	0.23–0.34	7.3
A1656	0.36–0.47[c]	9.3
A1795	0.20–0.40	8.5
A2199	0.12–0.16	6.7

[a] In Mpc from Jones and Forman 1984.
[b] At 2 Mpc in units of $10^{14}\ M_\odot$.
[c] Abramopoulos, Chanan, and Ku 1981.

approximately 125 h_{50}^{+1} for Coma and Perseus within 2 h_{50}^{-1} Mpc compared to Kent and Sargent's (1983) best values from the optical data of 160 h_{50} for Coma and 300 h_{50} for Perseus. With a more probable choice of parameters (see § V [eg. $\gamma = 1.37$, $T_0 = 15$ keV, $\delta = 1.14$ for Coma], the values are considerably lower, with best-fit values of ~ 90 for M/L_v in Coma at 2 h_{50}^{-1} Mpc. An interesting point about the mass-to-light ratios is their peak within the core followed by a relatively constant value at larger radii. We shall show in the next section that this is not simply an artifact of the polytropic assumption but a fairly direct consequence of the X-ray data combined with the assumption of a King light profile in the central regions.

It is quite probable that the innermost regions of clusters are not well described by a King model (e.g., Quintana 1979; Beers and Tonry 1986). To see whether the rise in M/L in the central regions of Coma is due to the artifact of an analytic King model assumption for the light distribution, we take the result of Quintana who shows that while in the central 0.2 h_{50}^{-1} Mpc there is an excess of light of 1.5–2 times the King model density, the King model is a good fit at larger radii. This effect would be to lower the central value of M/L to ~ 120 (see Fig. 4), the value seen at radii greater than 1 h_{50}^{-1} Mpc. It is thus entirely possible that there is not a rise in M/L in the central regions of clusters and that the galaxy light distribution is indeed steeper than a King profile. In this case we recover a constant M/L as a direct *consequence* of the X-ray data.

c) *Total Mass in Baryons*

The mass of gas in a cluster can be analytically calculated for a typical value, $\delta = 1$, as

$$M_{\rm gas}(<x) = 4.5 \times 10^{13}\ M_\odot\ (a/0.4\ {\rm Mpc})^3 \times (n_0/2 \times 10^{-3})(x - \tan^{-1} x)\ h_{50}^{-5/2}, \quad (19)$$

where n_0 is the central electron density of the gas in particles $\rm cm^{-3}$. For Coma at 2 Mpc $M_{\rm gas} \approx 1.6 \times 10^{14}\ M_\odot$. (If we use $\delta = 1.15$, $M_{\rm gas} = 1.16 \times 10^{14}\ M_\odot$.) If we use for the mass in stars a $M/L_v \approx 7$, appropriate for an elliptical galaxy (Pickles 1985), then the mass in stars inside 2 h_{50}^{-1} Mpc is $M_* \approx 6 \times 10^{13}\ M_\odot$ giving a total baryonic mass of $2.25 \times 10^{14}\ M_\odot$ at 2 Mpc. The baryons thus contribute at *least* 20% (16% if $\gamma = 1.15$) of the total mass inside this radius. Therefore the M/L_v of the "dark matter" in Coma is $\lesssim 99$. As an extremum for the "minimum" allowed virial mass and M/L_v we take the $\phi = 0.46$ case which gives a mass of $7.2 \times 10^{14}\ M_\odot$ and a total M/L_v for Coma of 44, for Abell's largest allowed luminosity, and a M/L_v for the "dark matter" of *only* ~ 30. It is thus not inconsistent to state that the dark matter in clusters (at least Coma) maybe quite similar in form to that postulated for the disk of spiral galaxies (van Albada *et al.* 1985).

IV. GENERALIZED MODELS

An alternative approach to the problem is to assume a mass profile and then to use the hydrostatic equation to determine the temperature profile (this method is similar to that of Sarazin and Bahcall 1977). One may then test if the integrated spectrum is an acceptable fit to the data. This method has the "virtue" of making no *a priori* assumptions about the functional form of the temperature profile.

For this case it is simplest to use the hydrostatic equation in the form,

$$T = (1 + x^2)^{\delta}\left[\frac{T_R}{(1 + x_R^2)^{\delta}} + \frac{\bar{m}G}{ka}\int_x^{x_R} \frac{M_V(x)}{x^2(1 + x^2)^{\delta}}\,dx\right], \quad (20)$$

where T_R is the temperature at a reference radius x_R.

First, consider the case of constant M/L ratio models where the luminosity has the analytic King model form of equation (18). This integration is shown in Figure 2 for Coma with

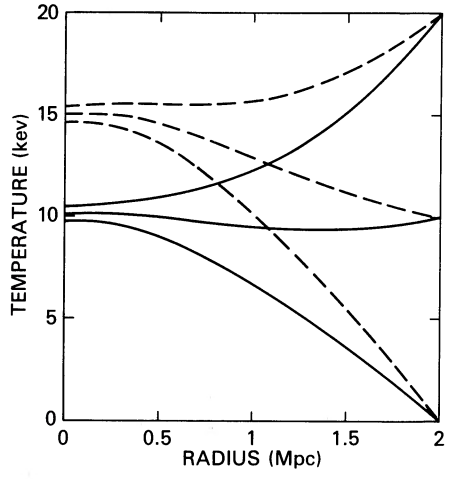

FIG. 2a

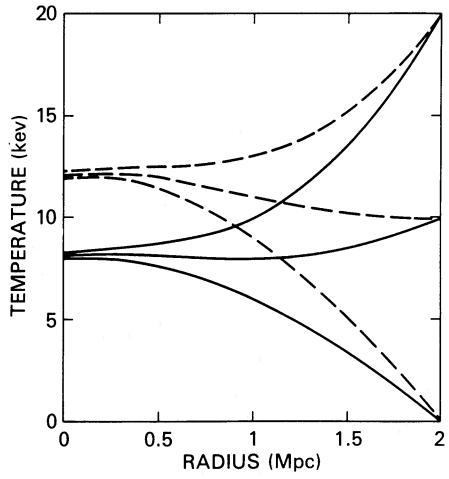

FIG. 2b

FIG. 2.—(*a*) The distribution of temperature vs. radius for Coma for a $\delta = 1$ model. The solid line is for the case of $M/L_V = 100$ and the dotted line for $M/L_V = 150$. (*b*) The distribution of temperature vs. radius for Coma for a $\delta = 1.25$ model. The solid line is for the case of $M/L_V = 100$ and the dotted line for $M/L_V = 150$.

$a = 0.34\ h_{50}^{-1}$ Mpc and $b = 0.37\ h_{50}^{-1}$ Mpc for the cases $\delta = 1.0$ an $\delta = 1.25$, for $M/L_V = 100$ and 150, and for $T_R = 0$, 10 and 20 keV at $2\ h_{50}^{-1}$ Mpc.

The integrated spectra of these models appear very nearly isothermal since the temperature profiles in the core regions are much shallower than those of the best-fitting polytropes. If the integrated spectra are force-fitted to the *HEAO 1* data, they give $M/L_V \approx 110\ h_{50}$ for $\delta = 1.25$, but they are not acceptable fits.

In order to obtain a better fit to the spectrum, we need a steeper temperature profile in the central regions, which in turn requires additional mass in the core regions. Inclusion of such additional mass produces mass distributions similar to those of the polytropic models of Figure 1, with high mass-to-light ratios in the core and relatively constant values outside. The required excess core mass in Coma is about $1\text{–}2 \times 10^{13}\ h_{50}\ M_\odot$, and the mass-to-light ratio is about $100\ h_{50}^{+1}$ beyond the core. We thus recover the results derived from the polytropic model by this different route.

V. OPTICAL VELOCITY DISPERSIONS

So far we have not considered whether the models of the previous two sections are consistent with the optical velocity

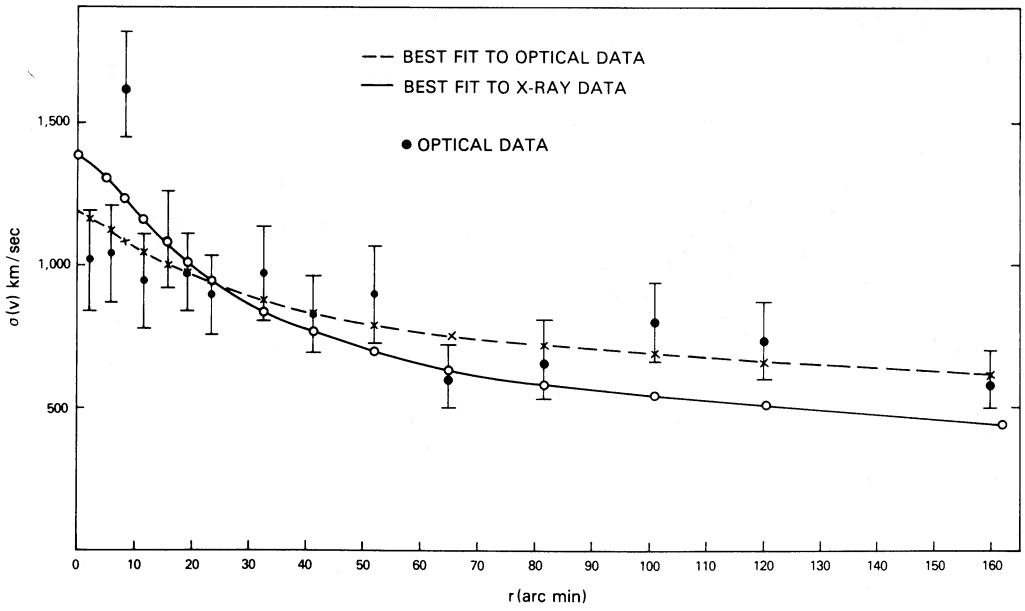

FIG. 3*a*

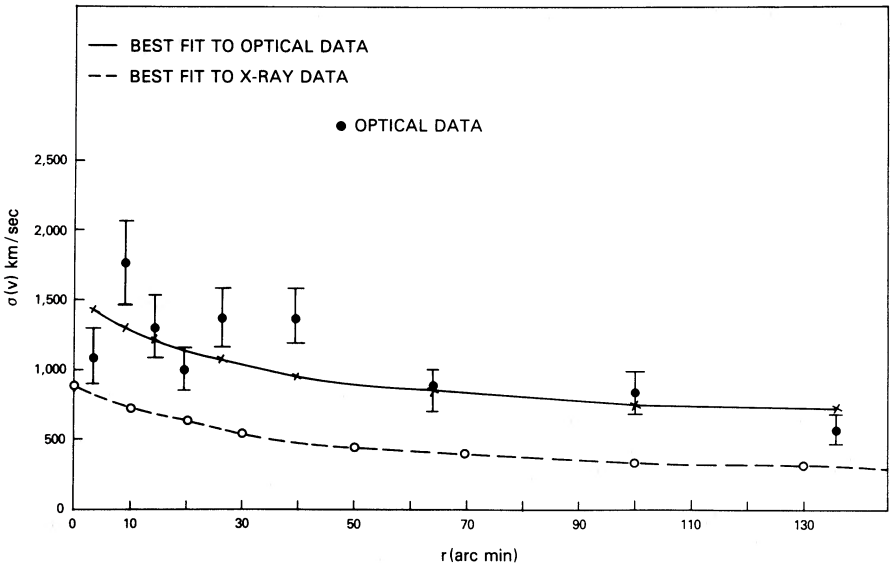

FIG. 3*b*

FIG. 3.—(*a*) The velocity dispersion vs. radius for Coma for the best-fit polytropic models (*solid line* for the model that best fits the X-ray data, *dotted line* for the best fit to the optical data only) vs. the data points of Kent and Gunn. (*b*) The velocity dispersion vs. radius for the Perseus cluster for the best-fit polytropic models (*solid line* for the model that best fits the X-ray data, *dotted line* for the best fit to the optical data only) vs. the data points of Kent and Sargent.

dispersion data. It is simplest for this purpose to use the analytic form of equation (11) which we now write in the form

$$M_V = M_0 \frac{x^3}{(1+x^2)^{(1+\phi)}}, \tag{21}$$

where $M_0 = 2\delta\gamma(kaT_0/G\bar{m})$ and $x = r/a$. Now assuming the velocity distribution of the galaxies is isotropic, and the galaxies are in hydrostatic equilibrium in the potential well of the cluster, the light-weighted projected velocity dispersion at projected radius p (where p is in core radii) is given by

$$\sigma_p^2(p) = \frac{GM_0}{a} \frac{\int_p^\infty [x/(1+x^2)^{1+\phi}] \times [(x^2-p^2)^{1/2}/(1+B^2x^2)^{3/2}]}{\int_p^\infty [1/(x^2-p^2)^{1/2}][x/(1+B^2x^2)^{3/2}]} dx,$$

which for Coma, where $B \approx 1$, may be simply integrated to give

$$\sigma_p^2 = \frac{\sqrt{\pi}}{(2\phi+3)} \frac{\Gamma(\phi+1)}{\Gamma(\phi+3/2)} \frac{\gamma\delta kT_0}{\bar{m}} (1+p^2)^{-\phi}. \tag{22a}$$

The ratio of the ϕ-dependent functions is approximately constant over the interesting domain of ϕ, and we can thus write

$$\sigma_p \approx 866(\gamma\delta)^{1/2}(T/10)_{\rm keV}^{1/2}(1+p^2)^{-\phi} \text{ km s}^{-1}. \tag{22b}$$

As can be seen from Figure 3*a*, the models at the low end of the γ and δ values determined from the X-ray data provide a very good fit to Coma's velocity dispersion profile while higher values do not. The allowed values from optical data only for Coma have $6.8 \lesssim T_0 \lesssim 15.8$ and $1.1 \lesssim \gamma \lesssim 1.34$ and thus only marginally overlap the X-ray best fits (Henriksen and Mushotzky 1986*a*). "Isothermal models" do not provide a good fit either. Of course the appropriate "King" models (Kent and Gunn 1982) can fit the velocity data. The intersection of the best-fit values for both optical and X-rays is small and rather marginally acceptable as regards the X-ray data. If we fit the Coma optical data within the region where the X-ray data provide any constraints (< 9 core radii or 3.6 Mpc) then the optical data can be well fit (reduced $\chi^2 < 1.5$) with parameters [$\delta = 0.9$, $\gamma = 1.4$ and $T(0) = 18$ keV] which are entirely consistent with the X-ray data alone. Using the largest γ and T_0 (at 68% confidence) from the optical data alone, we obtain the mass-to-light profile shown in Figure 4. Again, the mass-to-light ratios have the extremely interesting property of being constant at larger radii and have asymptotic values of 100–125 h_{50}.

None of the models provide a particularly good fit to the Perseus cluster data—the central velocity dispersion is always too high (Fig. 3*b*). This is a notorious problem in Perseus and is usually attributed to anisotropy of the galaxy velocity distribution in the core (e.g., Kent and Sargent 1983 and references therein). Because we have assumed isotropic galaxy orbits the magnitude of the temperature discrepancy is almost exactly the same as that found by Kent and Sargent (1983), a factor of 2. We note that if we renormalize the central velocity dispersion by this factor, the predicted trend of velocity dispersion with radius follows the optical data quite well. Another explanation might be the presence of a foreground clump of high-velocity galaxies projected on the core of Perseus.

The only other cluster which has sufficiently high-quality optical data to attempt a fit even for $\sigma_p(0)$ is Abell 2199. In this case the combined optical and X-ray data have small allowed boundaries (Henriksen and Mushotzky 1986*b*) with $5.0 \lesssim T_0 \lesssim 5.8$ keV and $1.1 \lesssim \gamma \lesssim 1.2$.

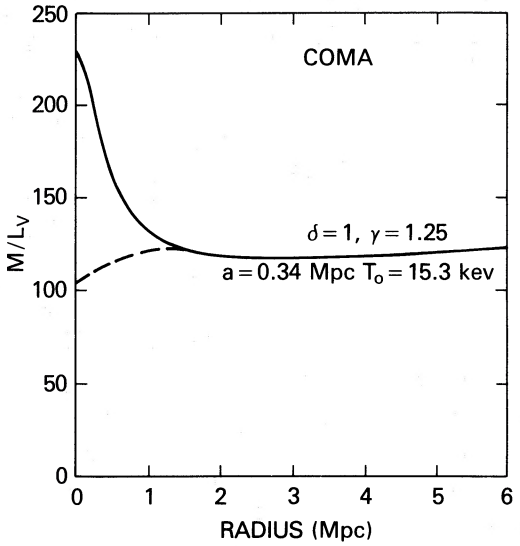

FIG. 4.—The mass-to-light ratio for Coma vs. radius using a $\delta = 1.0$, $\gamma = 1.25$, $T_0 = 15.3$ keV model. Notice the rise in the center and the flatness of M/L vs. radius at large distances. The dashed line indicates a possible M/L value if the central 0.5 Mpc of Coma is better described by a power law (Tonry and Beers) galaxy distribution.

The general agreement of optical and X-ray data for Coma and Abell 2199 seem to rule out gross anisotropies in the orbits of the galaxies which, however, seems to be required for Perseus.

VI. CONCLUSIONS

Our final conclusion is that the X-ray data cannot accept high mass-to-light ratios in these clusters. Typical mass-to-light ratios must be less than 125 h_{50} on the basis of the X-ray data, and preferred values are considerably smaller. The range of acceptable values for Coma is 44–120 h_{50}. The optical data for Coma cannot accept the lower of these values however, and the intersection of the two data sets suggest $M/L \approx 100$–125 h_{50} for Coma.

Typically, the virial mass of the clusters at 2 h_{50}^{-1} Mpc lies around 10^{15} $M_\odot$. For Coma, extrapolating the gas profiles to this radius would give a gas mass of around 2×10^{14} $h_{50}^{-5/2}$ $M_\odot$. The residual mass in galaxies would correspond to a mass-to-light ratio of around 70 h_{50} if the gas were excluded. This remarkably low value would suggest that at least in the clusters, the dark mass of the galactic halos is not extremely large.

Finally, the present result should encourage us to revisit our thinking on whether $\Omega = 1$, since it removes one of the very few reasons to suppose that the mass-to-light ratio increases with scale size in the universe.

We thank Keith Arnaud for help in analyzing the Coma velocity profile. R. M. thanks the Institute of Astronomy, Cambridge, England for hospitality.

REFERENCES

Abell, G. 1977, *Ap. J.*, **213**, 327.
Abramopoulos, F., Chanan, G., and Ku, W. H. 1981, *Ap. J.*, **248**, 429.
Abramopoulos, F., and Ku, W. H. 1983, *Ap. J.*, **271**, 446.
Bailey, M. E. 1982, *M.N.R.A.S.*, **201**, 271.
Beers, T., and Tonry, J. 1986, *Ap. J.*, **300**, 557.
Cavaliere, A. 1980, in *X-ray Astronomy*, ed. R. Giacconi and G. Setti (Reidel: Dordrecht), p. 217.
Cavaliere, A., and Fusco-Femiano, R. 1976, *Astr. Ap.*, **49**, 137.
Fabian, A., Hu, E. M., Cowie, L. L., and Grindlay, J. 1981, *Ap. J.*, **248**, 47.
Fabricant, D. M., and Gorenstein, P. 1983, *Ap. J.*, **267**, 535.
Fabricant, D. M., Lecar, M., and Gorenstein, P. 1980, *Ap. J.*, **241**, 552.
Felten, J. 1985, *Comments Ap.*, **11**, 53.
———. 1986, in *IAU Symposium 118, Dark Matter in the Universe*, ed. G. Knapp and J. Kormendy (Dordrecht: Reidel), in press.
Henriksen, M., and Mushotzky, R. 1986*a*, *Ap. J.*, **302**, 287.
———. 1986*b*, *Ap. J.*, submitted.
Jones, C., and Forman, W. 1984, *Ap. J.*, **276**, 38.
Kent, S. M., and Gunn, J. E. 1982, *A.J.*, **87**, 945.
Kent, S. M., and Sargent, W. L. 1983, *A.J.*, **88**, 697.
Mushotzky, R. F. 1984, *Phys. Scripta*, **T7**, 157.
Pickles, A. J. 1985, *Ap. J.*, **296**, 340.
Quintana, H. 1979, *A.J.*, **84**, 15.
Rood, H. S. 1981, *Rep. Prog. Phys.*, **44**, 1081.
Rybicki, G., Gorenstein, P., and Fabricant, D. M. 1984, *Ap. J.*, **286**, 186.
Sarazin, C. L. 1985, *Rev. Mod. Phys.*, in press.
Sarazin, C., and Bahcall, J. 1977, *Ap. J. Suppl.*, **34**, 451.
Stewart, G. C., Canizares, C. R., and Nulsen, P. E. J. 1984, *Ap. J.*, **278**, 536.
van Albada, T. S., Bahcall, J., Begeman, K., and Sancisi, R. 1985, *Ap. J.*, **295**, 305.

LENNOX L. COWIE: Institute of Astronomy, University of Hawaii, Honolulu, HI 96822

MARK HENRIKSEN: Space Telescope Science Institute, Homewood Campus, The Johns Hopkins University, Baltimore, MD 21218

RICHARD MUSHOTZKY: Laboratory for High Energy Astrophysics, Code 666, Goddard Space Flight Center, Greenbelt, MD 20771